

Reduction of the amplified spontaneous emission threshold in semiconducting polymer waveguides on porous silica.

Fernando Lahoz,^{1*} Claudio J. Oton,² Nestor Capuj,³ Miriam Ferrer-González,¹ Stephanie Cheylan,⁴ and Daniel Navarro-Urrios⁵

¹ *Departamento Física Fundamental y Experimental, Electrónica y Sistemas-Instituto Universitario de Estudios Avanzados en Física Molecular, Atómica y Fotónica, Universidad de La Laguna, 38206 La Laguna, Tenerife, Spain.*

² *Optoelectronics Research Centre, University of Southampton, Southampton, SO17 1BJ, UK.*

³ *Departamento Física Básica, Universidad de La Laguna, E-38206 La Laguna, Tenerife, Spain.*

⁴ *ICFO- Institut de Ciències Fotòniques, 08860 Castelldefels, Barcelona, Spain.*

⁵ *MIND-IN2UB, Dept. Electrònica, Universitat de Barcelona, Martí i Franquès 1, 08028 Barcelona, CAT, Spain.*

**flahoz@ull.es*

Abstract: Hybrid organic-inorganic monomode waveguides of conjugated polymers on porous silicon (PS) substrates have been fabricated. Different low refractive index PS substrates, varying from 1.46 down to 1.18 have been studied. Amplified spontaneous emission (ASE) has been observed for all the samples and the ASE threshold has been monitored as a function of the PS refractive index. A decrease in the ASE threshold is detected when the PS refractive index decreases. These results have been analysed in the frame of a four level waveguide amplifier model and the theoretical predictions are in agreement with the experimental data.

©2009 Optical Society of America

OCIS codes: (130.3120) Integrated optics devices; (130.5460) Polymer waveguides.

References and links

1. J. H. Burroughes, D. D. C. Bradley, A. R. Brown, R. N. Marks, K. Mackay, R. H. Friend, P. L. Burn, and A. B. Holmes, "Light-Emitting Diodes Based on Conjugated Polymers," *Nature* **347**(6293), 539–541 (1990).
2. N. Tessler, "Lasers Based on Semiconducting Organic Materials," *Adv. Mater.* **11**(5), 363–370 (1999).
3. I. D. W. Samuel, and G. A. Turnbull, "Organic semiconductor lasers," *Chem. Rev.* **107**(4), 1272–1295 (2007).
4. I. D. W. Samuel, and G. A. Turnbull, "Polymer lasers: recent advances," *Mater. Today* **7**(9), 28–35 (2004).
5. M. Reufer, J. Feldmann, P. Rudati, A. Rühl, D. Müller, K. Meerholz, C. Karnutsch, M. Gerken, and U. Lemmer, "Amplified spontaneous emission in an organic semiconducting multilayer waveguide structure including a highly conductive transparent electrode," *Appl. Phys. Lett.* **86**(22), 221102 (2005).
6. G. A. Turnbull, P. Andrews, W. L. Barnes, and I. D. W. Samuel, "Operating characteristics of a semiconducting polymer laser pumped by a microchip laser," *Appl. Phys. Lett.* **82**(3), 313–315 (2003).
7. C. Karnutsch, C. Gyrtner, V. Haug, U. Lemmer, T. Farrell, B. S. Nehls, U. Scherf, J. Wang, T. Weimann, G. Heliotis, C. Pflumm, J. C. deMello, and D. D. C. Bradley, "Low threshold blue conjugated polymer lasers with first- and second-order distributed feedback," *Appl. Phys. Lett.* **89**(20), 201108 (2006).
8. T. Riedl, T. Rabe, H. H. Johannes, W. Kowalsky, J. Wang, T. Weimann, P. Hinze, B. Nehls, T. Farrell, and U. Scherf, "Tunable organic thin-film laser pumped by an inorganic violet diode laser," *Appl. Phys. Lett.* **88**(24), 241116 (2006).
9. Y. Yang, G. A. Turnbull, and I. D. Samuel, "Hybrid optoelectronics: A polymer laser pumped by a nitride light-emitting diode," *Appl. Phys. Lett.* **92**(16), 163306 (2008).
10. G. Heliotis, S. A. Choulis, G. Itskos, R. Xia, R. Murray, P. N. Stavrinou, and D. D. C. Bradley, "Low-threshold lasers based on a high-mobility semiconducting polymer," *Appl. Phys. Lett.* **88**(8), 081104 (2006).
11. E. B. Namdas, M. Tong, P. Ledochowitsch, S. R. Mednick, J. D. Yuen, D. Moses, and A. J. Heeger, "Low threshold in polymer lasers on conductive substrates by distributed feedback nanoimprinting: Progress toward electrically pumped plastic lasers," *Adv. Mater.* **21**(7), 799–802 (2009).
12. F. Laquai, A. K. Mishra, K. Müllen, and R. H. Friend, "Amplified Spontaneous Emission of Poly(ladder-type phenylene)s—The Influence of Photophysical Properties on ASE Thresholds," *Adv. Funct. Mater.* **18**(20), 3265–3275 (2008).
13. G. Heliotis, R. D. Xia, G. A. Turnbull, P. Andrew, W. L. Barnes, I. D. W. Samuel, and D. D. C. Bradley, "Emission characteristics and performance comparison of polyfluorene lasers with one- and two-dimensional distributed feedback," *Adv. Funct. Mater.* **14**(1), 91–97 (2004).

14. C. Karnutsch, C. Pflumm, G. Heliotis, J. C. deMello, D. D. C. Bradley, J. Wang, T. Weimann, V. Haug, C. Gärtner, and U. Lemmer, "Improved organic semiconducting lasers based on a mixed-order distributed feedback resonator design," *Appl. Phys. Lett.* **90**(13), 131104 (2007).
15. I. B. Martini, I. M. Craig, W. C. Molenkamp, H. Miyata, S. H. Tolbert, and B. J. Schwartz, "Controlling optical gain in semiconducting polymers with nanoscale chain positioning and alignment," *Nat. Nanotechnol.* **2**(10), 647–652 (2007).
16. A. G. Cullis, L. T. Canham, and P. D. J. Calcott, "The structural and luminescence properties of porous silicon," *J. Appl. Phys.* **82**(3), 909–965 (1997).
17. E. Lorenzo, C. J. Oton, N. E. Capuj, M. Ghulinyan, D. Navarro-Urrios, Z. Gaburro, and L. Pavesi, "Porous silicon-based rugate filters," *Appl. Opt.* **44**(26), 5415–5421 (2005).
18. P. Ferrand, D. Loi, and R. Romenstein, "Photonic band-gap guidance in high-porosity luminescent porous silicon," *Appl. Phys. Lett.* **79**(19), 3017–3019 (2001).
19. M. Ghulinyan, C. J. Oton, G. Bonetti, Z. Gaburro, and L. Pavesi, "Free-standing porous silicon single and multiple optical cavities," *J. Appl. Phys.* **93**(12), 9724–9729 (2003).
20. F. Lahoz, N. Capuj, C. Oton, and S. Cheylan, "Optical gain in conjugated polymer hybrid structures based on porous silicon waveguides," *Chem. Phys. Lett.* **463**(4-6), 387–390 (2008).
21. C. J. Oton, E. Lorenzo, N. Capuj, F. Lahoz, I. R. Martin, D. Navarro-Urrios, M. Ghulinyan, F. Sbrana, Z. Gaburro, and L. Pavesi, "Porous silicon-based Notch filters and waveguides," *Proc. SPIE Int. Soc. Opt. Eng.* **5840**, 434–443 (2005).
22. P. K. Tien, "Light waves in thin films and integrated optics," *Appl. Opt.* **10**(11), 2395 (1971).
23. M. Yan, L. J. Rothberg, E. W. Kwock, and T. M. Miller, "Interchain excitations in conjugated polymers," *Phys. Rev. Lett.* **75**(10), 1992–1995 (1995).
24. K. Koynov, A. Bahtiar, T. Ahn, C. Bubeck, and H. H. Horhold, "Molecular weight dependence of birefringence of thin films of the conjugated polymer poly[2-methoxy-5-(2-ethyl-hexyloxy)-1, 4-phenylenevinylene]," *Appl. Phys. Lett.* **84**(19), 3792–3794 (2004).
25. M. D. McGehee, R. Gupta, S. Veenstra, E. K. Miller, M. A. Diaz-Garcia, and A. J. Heeger, "Amplified spontaneous emission from photopumped films of a conjugated polymer," *Phys. Rev. B* **58**(11), 7035–7039 (1998).
26. M. D. McGehee, and A. J. Heeger, "Semiconducting (conjugated) polymers as materials for solid-state lasers," *Adv. Mater.* **12**(22), 1655–1668 (2000).
27. J. Chilwell, and I. Hodgkinson, "Thin-films field-transfer matrix-theory of planar multilayer waveguides and reflection from prism-loaded waveguides," *J. Opt. Soc. Am. A* **1**(7), 742–753 (1984).
28. C. M. Heller, I. H. Campbell, B. K. Laurich, D. L. Smith, D. D. C. Bradley, P. L. Burn, J. P. Ferraris, and K. Müllen, "Solid-state-concentration effects on the optical absorption and emission of poly(p-phenylene vinylene)-related materials," *Phys. Rev. B* **54**(8), 5516–5522 (1996).
29. J. P. Schmidtke, J. S. Kim, J. Gierschner, C. Silva, and R. H. Friend, "Optical spectroscopy of a polyfluorene copolymer at high pressure: intra- and intermolecular interactions," *Phys. Rev. Lett.* **99**(16), 167401 (2007).
30. E. M. Calzado, J. M. Villalvilla, P. G. Boj, J. A. Quintana, and M. A. Diaz-Garcia, "Concentration dependence of amplified spontaneous emission in organic-based waveguides," *Org. Electron.* **7**(5), 319–329 (2006).
31. G.- Wegmann, B. Schweitzer, M. Hopmeier, M. Oestreich, H. Giessen, and, and R. F. Mahrt, "., "Conjugated polymer lasers: emission characteristics and gain mechanism," *Phys. Chem. Chem. Phys.* **1**(8), 1795–1800 (1999).
32. R. Gupta, J. Stevenson, A. Dogariu, M. D. McGehee, J. Y. Park, V. Sradanov, A. J. Heeger, and H. Wang, "Low-threshold amplified spontaneous emission in blends of conjugated polymers," *Appl. Phys. Lett.* **73**(24), 3492–3494 (1998).

1. Introduction

Since the pioneering work of Burroughes et al. [1] in 1990, in which polymer based organic light emitting diodes were reported, these materials have attracted much interest for their optoelectronics applications such as gain media for lasers and optical amplifiers [2]. The use of polymers for the fabrication of lasers and/or optical amplifiers is especially attractive because they can provide versatile, flexible and cheap light sources that show the ability to easily tune their emission wavelength over a large spectral range through the modification of their molecular structure [3]. Laser emission and broad band amplification have already been reported in semiconductor polymers under optical pumping [4,5]. However, neither laser emission nor optical amplification have been achieved under electrical pumping yet, because of the high current densities that are required to obtain a positive gain medium and the additional losses due to the interaction of the laser mode with the electrodes required for charge injection. An alternative approach recently proposed in order to overcome the difficulties of direct electrical pumping of a semiconducting polymer consist in using small and compact pump sources such as a microchip laser to achieve the necessary population

inversion for laser operation [6–9]. In both cases, either under direct electrical pumping or by the use of compact microchip laser sources, the reduction of the laser threshold is one of the most desirable characteristics that would actually make the fabrication of polymer based electrooptical devices a more realistic target.

Novel semiconducting polymers have been reported to show low thresholds for laser emission [10,11], and amplified spontaneous emission (ASE), which is usually considered as the first test for a laser medium. It has been shown that the chemical structure of the organic material has an important influence on the optical amplification properties of the material [12]. All these reports seem to indicate that chemical engineering could be a promising route to further improve the optical characteristics of conjugated polymers.

An alternative way to reduce the laser threshold that is actively investigated in different laboratories is focused on the design of improved optical structures. For instance, low-threshold optically pumped conjugated polymer lasers have been obtained using distributed feedback (DFB) resonators [13,14]. A recent investigation has shown a reduction in the ASE threshold that is independent on the chemical structure of the polymer and it is based on the encapsulation of the semiconducting polymer in nanopores of a silica host [15].

In order to investigate the ASE threshold of semiconducting polymers, we have fabricated waveguide structures based on one of the most frequently used conjugated polymers, poly(2-methoxy-5-(2'-ethyl-hexyloxy)-1,4-phenylene vinylene) (namely MEH-PPV), deposited on porous silicon (PS). The waveguide structure provides the confinement of the light in the polymer layer, which enhances the stimulated emission of light and obtain optical amplification. PS can be easily obtained on silicon by electrochemical etching [16]. Despite the high refractive index of silicon ($n \sim 3.5$), low refractive index layers of PS can be easily obtained when the porosity of the film is increased, enabling the direct deposition of a core layer on the PS cladding. Moreover, the porosity of this material can be changed in depth with an arbitrary profile, allowing modulation of the refractive index and the fabrication of different photonic structures, such as filters [17], waveguides [18], and resonators [19]. In fact, we have recently reported on the first achievement of optical amplification in a high index contrast hetero-structure waveguide formed by a core layer of Poly[2-methoxy-5-(3',7'-dimethyloctyloxy)-1,4-phenylenevinylene] (MDMO-PPV) emissive conjugated polymer deposited on an oxidized PS substrate [20].

In this paper, we report on the effect of the control of the refractive index of the PS substrate on the ASE threshold of the emissive polymer. By changing the porosity of the PS cladding the refractive index can be tuned at different values. A reduction of the ASE threshold is observed when the refractive index of the PS layer is decreased. A reasonable agreement between the experimental data and the theoretical predictions for a four-level waveguide amplifier model is found. Moreover, the use of these PS hybrid waveguide structures is discussed for other emissive organic materials and the influence on the ASE threshold is predicted.

2. Experimental details

A 5 μm PS layer was formed by electrochemical etching of (100)-oriented heavily doped (0.01 Ωcm resistivity) p-type silicon. Different current densities, in the range of 20 to 80 mA/cm^2 have been applied to a 1 cm^2 Si circular area in order to tune the refractive index of the PS layer. PS strongly absorbs in the visible range and, in order to have transparent substrates, the samples were annealed at 900°C in air for 3 hours to oxidize the silicon skeleton, and convert it into transparent porous silica. The oxidation process further reduces the refractive index. (A detailed characterization of the refractive index of the PS thin films can be found in [21]. Three different porous silica samples were prepared with refractive index values of 1.46, 1.33 and 1.18, which will be labeled as samples 1, 2, and 3, respectively in the text. The mean pore size for sample 3 is around 10-15 nm and decreases as n increases.

In sample 1 the pores collapse and dense silica thin film is obtained. The small size of the pores prevents any important penetration of the polymer chains into the substrate.

MEH-PPV (Aldrich) was dissolved in toluene at a concentration of 10 mg/ml and the final solution was filtered. Thin films were prepared from the toluene based-solution via spin-coating on the PS layers. The waveguides were designed to be single-mode. The spin-cast films are rather uniform except near the edge of the substrate. In order to have a good edge quality, we cleaved the silicon substrate, which enables to out-couple the waveguided PL from the end-facet.

The waveguide characterization was performed with a prism-coupling setup. A Gadolinium Gallium Garnet prism (GGG, index 1.965) was pressed against the layers, and the beam of a He-Ne laser (633 nm) was directed to the coupling spot. The reflected signal was collected as a function of the incident angle θ , and the result was plotted versus effective index, which is defined as $n_p \sin(\theta)$, being n_p the index of the prism. This plot allows us to directly measure the effective index of the modes (through the so-called *dark m-lines*) and the refractive index of the bottom cladding (at the point where the total internal reflection region finishes) [22].

The samples were placed in a chamber with flowing argon in order to avoid photo oxidation of the polymers. An optical parametric oscillator (OPO) tunable pulsed laser, with 10 ns pulses, was used as the excitation source. The typical decay time of the PL of MEH-PPV polymer thin films is in the range of a few hundreds of picoseconds [23]. Therefore, we can assume that the PL of the system reaches a stationary regime under OPO laser pulses of 10 ns of duration. A cylindrical lens system focused the pump beam on the waveguide to form a horizontal line which had a width of about 300 μm . An adjustable slit was placed in front of the waveguide in order to vary the illumination length on the waveguide. A fiber coupled CCD spectrometer was used to record the PL spectra through the cleaved end-facets.

3. Experimental results and discussion

3.1 Waveguiding characteristics

Figure 1 shows the prism coupling curves performed for the TE polarization, where the total internal reflection region and the cladding region (below the critical angle) are easily distinguishable. The fringe pattern observed in the latter is due to the interference produced by the bottom cladding, which is only 5 microns thick. The refractive index of the PS layers was extracted from these curves, and corresponds to the values shown in Table 1. The fact that we only observed one peak in the total internal reflection region means that all the waveguides are single mode. The value of the waveguide effective index was used to calculate the refractive index of the core layer by using the thickness value from profilometry measurements. In all cases, the calculated core refractive index was about 1.81, which agrees with previous reports [22]. No TM guided mode was observed except for sample 3, which had the highest index contrast. This implies that the waveguide core is very birefringent. Our estimation is that birefringence is negative (ordinary index > extraordinary index) and higher than 10%, which has been previously reported too [24].

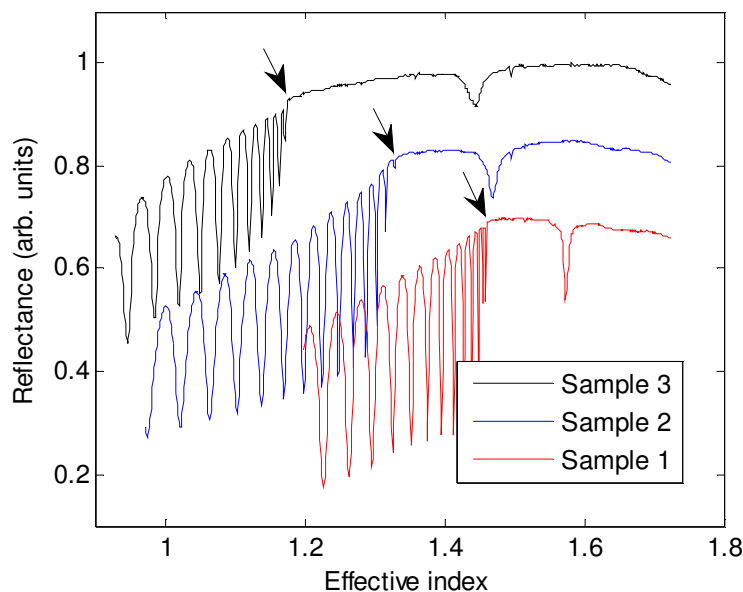


Fig. 1. Dark m-line spectra showing the TE reflectance through a high index prism varying the incidence angle (*i.e.* the effective index). Samples 3 (black), 2 (blue) and 1 (red) with different PS refractive indices are shown. The arrows indicate the PS refractive index in each case, and the isolated peaks show the effective index of the waveguide.

3.2 Guided photoluminescence and ASE experiments

Due to the high density of chromophores in the polymer layer, MEH-PPV shows a strong absorption coefficient. A thin film of MEH-PPV was deposited on a transparent glass substrate in order to perform an optical absorption measurement. The optical absorption coefficient, α , is given in the inset of Fig. 2.a. The maximum absorption is centered at about 500 nm and this value was chosen for the OPO excitation wavelength of the PL spectra.

The guided PL of the samples has been detected through the cleaved edge when the samples were excited with pulses at 500 nm. In all the cases we have observed a clear narrowing of the emission spectra when the energy of the pump pulses is increased above a certain threshold. These results are given in Fig. 2.a, when the excitation beam was focused on an about 1 mm length line on the waveguide. This narrowing of the luminescence spectra is the main feature of ASE. On the other hand, no narrowing of the PL spectra was observed at any pump energies when the same polymer were deposited on crystalline Si ($n = 3.5$), for which no waveguiding structure exists and, besides, strong absorption due to Si contributes to prevent ASE. This indicates that the confinement of the PL in the core layer of the waveguide is necessary in order to obtain optical amplification. In addition to this, we have measured the guided photoluminescence of the polymer as a function of the stripe length of the focused excitation beam on the polymer surface at a pump power above the ASE threshold. The results are given in Fig. 2.b. When the illumination length is very small (around 50 μm), the characteristic broad emission band of the polymer is recorded. However, when the illumination length is increased, a clear narrowing of the luminescence band is appreciated. This feature further confirms that the observed narrowing of the luminescence is due to ASE [25]. In fact, the narrowing effect is due to stimulated emission. Below threshold, emission is dominated by spontaneous decay, therefore it has the shape of the emission cross section profile. But above threshold, when the excitation stripe length is long enough to produce non-negligible amplification, stimulated emission becomes higher than spontaneous emission and

the spectrum gets narrower due to the exponential dependence of the output versus the excitation length. Moreover, the ASE peak wavelength slightly redshifts as the illumination length increases because the internal gain of the polymer already saturates at short illumination length while the losses due to the absorption tail of the polymer increase with length.

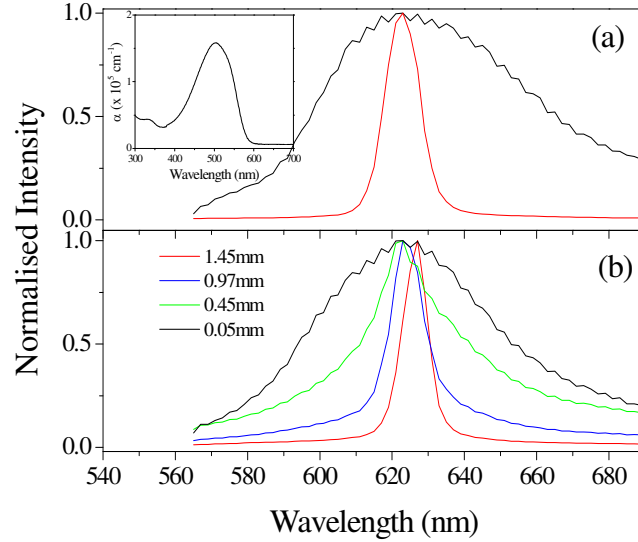


Fig. 2. (a) Normalized emission spectra of sample 3 above and below the ASE threshold. The inset shows the optical absorption coefficient of the MEH-PPV polymer. (b) Normalized emission spectra of sample 3 at a pump power above the ASE threshold as a function of the excitation stripe length.

We have measured the output intensity of the waveguide as a function of the pump stripe length using a pump power density of about 25 kW/cm^2 , well above the ASE threshold. In particular, we have performed this experiment for two different wavelengths, one at the peak of the emission spectrum at 627 nm and another at a lower wavelength, 585 nm, for which no narrowing of the luminescence due to ASE is observed. The results are given in Fig. 3. In the first case, a superlinear growth of the emission intensity is detected, while a sublinear behaviour is appreciated for the 585 nm emission wavelength. The dependence of the guided ASE signal, I_{ASE} , on the illumination length L is given by the equation:

$$I_{ASE} \propto \frac{1}{g} (e^{gL} - 1) \quad (1)$$

where g is the net modal gain. Figure 3 shows the best fitting of the experimental data to Eq. (1). A net positive gain of around 70 cm^{-1} was obtained for the ASE at 627 nm, which is similar to other reported values [25]. On the other hand, a negative value of about -3 cm^{-1} is obtained for the 585 nm emission wavelength. This is an expected result that indicates that ASE only happens at the peak of the emission band and the negative gain observed at 585 nm can be due to losses associated to the tail of the absorption band of the polymer.

The ASE pump power threshold is usually defined as the power at which the FWHM of the emission band is reduced to half. The evolution of the FWHM as a function of the power density of the pump pulses for samples 1, 2, and 3 is shown in Fig. 4. As it has already been

explained in the previous section, the ordinary refractive index of the polymer layer is 1.81 for the three samples. On the other hand, the refractive index of the PS cladding layers changes from sample 1 to 3. Sample 1 has an n value of 1.46, which is similar to quartz. In fact, fused quartz is often used as a transparent substrate to deposit conjugated polymers for optical applications [11]. When the porosity of the PS layer is increased, the refractive index decreases to 1.33, and 1.18 in samples 2, and 3, respectively. A monotonous reduction of the ASE threshold is observed as the n value of the cladding layer is decreased. The threshold changes from 8.1 kW/cm^2 in sample 1 to 6.2 kW/cm^2 in sample 3, which represents a reduction of about 22%. When the index contrast between the cladding and the core layer of the waveguide increases, the confinement of the guided mode in the core thin film becomes higher and, as a consequence, the probability of stimulated emission increases. This effect explains the reduction of the ASE threshold in the $n = 1.18$ cladding sample.

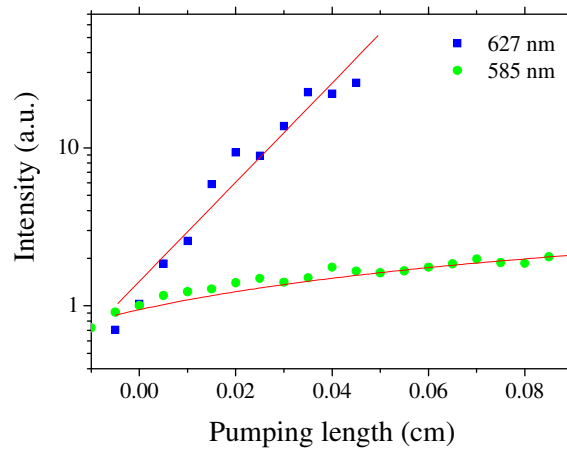


Fig. 3. ASE intensity at 627 nm (blue squares), and at 585 nm (green circles) as a function of the illumination length at a pump power density of about 25 kW/cm^2 . The fitting to the Eq. (1) is given by the red solid lines.

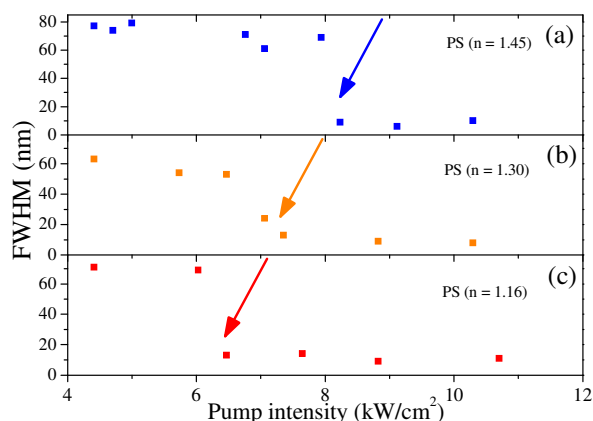


Fig. 4. Full width at half maximum of the emission band at different excitation powers for (a) sample 1, (b) 2, and (c) 3.

In order to quantify the expected reduction of the ASE threshold as a function of the confinement factor, we have considered a four-level waveguide amplifier system [26]. As a first approximation, the gain of a guided mode in such a system is given by:

$$g \approx \Gamma \sigma_e N^* - \alpha \quad (2)$$

where Γ is the confinement factor of the mode, σ_e the emission cross section, N^* the number of excited molecules per unit volume, and α includes all the loss mechanisms. We have to consider that the absorption coefficient at the pump wavelength is $1.5 \cdot 10^5 \text{ cm}^{-1}$, which leads to an absorption length of only 66 nm. The polymer layers are at least twice as thick and, as a first approximation, it will be considered that the excited region of the polymer film is limited to the first 66 nm in depth, and the excitation pump will be neglected for the rest of the active layer thickness. Within this simplified model, confinement of the guided mode has to be calculated as:

$$\Gamma \approx \frac{\int_0^\Lambda S dx}{\int_{-\infty}^\infty S dx} \quad (3)$$

where S is the Poynting vector of the mode and Λ the absorption length. Only the TE modes were considered, as the TM modes were not guided. The confinement factor was calculated for each sample by making use of a transfer matrix approach [27], using the measured parameters of refractive indices and thickness, and the results are shown in Table 1.

Table 1. Main optical parameter for samples 1, 2 and 3.

	Bottom cladding TE index	Thickness (nm)	Threshold (kW/cm ²)	Calculated Γ (first 66 nm)
Sample 1	1.4595	170	8.1	19.9%
Sample 2	1.325	127	7.0	27.7%
Sample 3	1.177	131	6.2	31.4%

If we assume that all the pump photons are absorbed along the effective absorption length, Λ , and that every photon absorbed generates an excited state, the excitation rate per unit volume in the excited region is equal to ϕ/Λ . Since we are under stationary conditions, as explained in Section 2, the rate of excitation must be equal to the rate of deexcitation per unit volume, therefore:

$$\frac{\phi}{\Lambda} = \frac{N^*}{\tau} \quad (4)$$

where τ denotes the total decay time of the excited chromophore. Therefore, to get the pump threshold for ASE, Eq. (2) needs to be equal to zero, which after substituting Eq. (4) gives:

$$\phi_{th} = \frac{\alpha\Lambda}{\Gamma\sigma_e\tau} \quad (5)$$

where ϕ_{th} denotes the pump flux at the threshold. Therefore, according to this analysis, the ASE threshold is inversely proportional to the confinement factor in the excited region.

Table 1 shows an obvious decreasing trend in the ASE threshold as the confinement factor increases. From the total confinement factor change between sample 1 and sample 3, an ASE threshold reduction of about 36% is theoretically expected according to Eq. (5). The experimentally observed ASE threshold reduction between those two samples is about 24%, which represents a reasonable agreement with the theory, taking into account the simplifications introduced in the model.

The relative increase of the confinement factor when the refractive index of the PS cladding layer decreases from 1.46 to 1.18 would be much higher for polymer core layers with an n value closer 1.46. In the case of MEH-PPV, n has a relatively high value of 1.81 which means that the confinement factor just experiences a moderate increase as the n parameter of the PS layer decreases. However, there is currently a practical interest in other lower refractive index polymer thin films. Indeed, different studies have been carried out to understand the nature of the photogenerated states in organic semiconductors trying to differentiate between inter- and intramolecular recombination processes and their influence on their optical properties and, eventually, the design of polymeric systems for optoelectronics [23,28,29]. One of the main conclusions of these studies is that interchain excitation is an important interaction mechanism in conjugated polymer thin films that can yield to migration to extrinsic, impurity related centers that compete with emissive intrachain exciton formation and reduce the efficiency. By increasing the separation between electronically active backbones intermolecular excitations are reduced and the quantum efficiency can be improved. In fact, a significant reduction in the ASE threshold has been reported when conjugated polymers are diluted in an inert matrix such as polystyrene or polymethylmethacrylate [30,31], or in blends of an absorbing host polymer and a small fraction of an emissive polymer [32]. In all these cases, the index values of the polymer blends are in the 1.5 to 1.6 range. In order to show how strong the ASE threshold reduction could be for this kind of polymer blends, we have simulated the mode profiles for a layer with index 1.55 on a PS cladding layer with index 1.46, or with index 1.18. Figure 5 shows the results, where the confinement factor varies from 33% to 80%, when the PS cladding layer decreases from 1.46 down to 1.18, respectively. According to our model the ASE threshold is expected to be reduced by a factor of 2.5 in the high confinement factor waveguide.

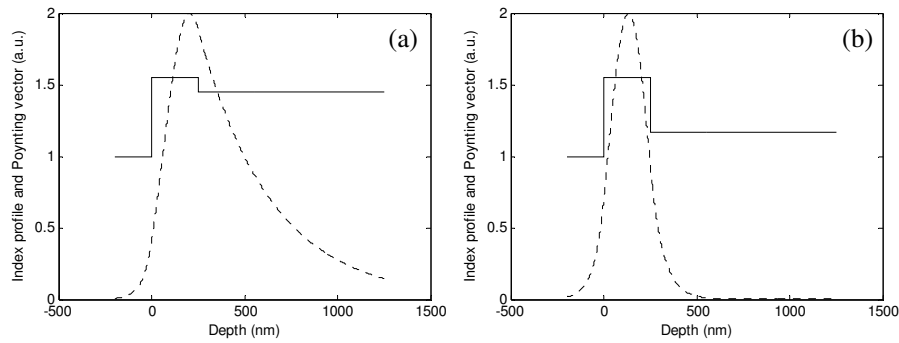


Fig. 5. Mode profiles for a 1.55-index 250nm-thick polymer waveguide with silica cladding with index 1.46 (a) and PS cladding with index 1.18 (b). The confinement factors assuming that all the active layer is excited are respectively 33% and 80%.

4. Conclusions

Hybrid organic-inorganic monomode waveguides have been fabricated. The emissive conjugated polymer MEH-PPV has been deposited onto PS substrates by spin-coating. Different refractive index substrates ranging from $n = 1.46$ down to 1.18 have been used by changing the porosity of the PS cladding. Evidence of ASE has been observed in all the cases. The pump power ASE threshold decreases when the refractive index of the PS layer is lower. A simple model based on a four-level waveguide amplifier has been used to explain the experimental results and a reasonable agreement between theory and experiments has been found. In fact, the decrease of the ASE threshold is due to the increase of confinement of the guided light in the polymer layer when the refractive index contrast with the PS cladding is higher. This model has also been used to predict an important ASE threshold reduction in diluted polymer blends, for which high confinement factors can be achieved on a low refractive index PS substrate.

Acknowledgements

We wish to thank the Spanish Ministry of Education and Science (MAT 2007-63319) and the Consolider-Ingenio (CSD2007-00007) for financial support. C. J. O. acknowledges support from the EU 6th framework program through an EIF Marie Curie Fellowship. S. C. also acknowledges support from the Spanish Ministry of Education and Science through the Ramon y Cajal program.